

Giuseppe Sappa<sup>18</sup>, Giulia Luciani<sup>19</sup>

## 6 Sensitivity of Dar Es Salaam Coastal Aquifer to Climate Change with Regard to Seawater Intrusion and Groundwater Availability

**Keywords:** Groundwater recharge, Seawater intrusion, Climate change

### 6.1 Introduction

This paper presents the initial results of three years of investigation activities, carried on in the Dar es Salaam coastal plain (Tanzania) by the Adapting to Climate Change in Coastal Dar es Salaam (ACC-DAR) project, a cofounded research project, granted by the European Union, led by the Sapienza, University of Rome, in cooperation with Ardhi University of Dar es Salaam. The ACC-DAR project activities will enhance the capacities of Dar's municipalities by increasing their understanding of adaptation practices, and by developing methodologies for integrating adaptation activities into strategies and plans for Urban Development and Environment Management (UDEM) in unplanned and unserved coastal settlements. In order to provide a series of enhanced methodologies for improving municipal activities related to climate change (CC) issues in the water management sector, the specific environmental phenomenon of seawater intrusion was investigated. This phenomenon is already contributing, and will increasingly contribute as CC progresses, to the degradation of those natural resources on which a large part of Dar es Salaam's peri-urban livelihoods depends. The target of this study was to investigate groundwater availability changes in Dar es Salaam's coastal aquifer as a consequence of seawater intrusion and urbanization processes in the framework of CC effects, with the aim to set up an integrated approach to evaluate CC effects on groundwater resources in coastal plains affected by seawater intrusion, and to better manage these important natural resources. As such, geological and hydrogeological characterization of the area is part of the study,

---

**18** Giuseppe Sappa is an Associate professor in Engineering Geology and Applied Hydrogeology at the Department of Civil, Building and Environmental Engineering, Sapienza University of Rome. He worked as Hydrogeologist Senior in ACC-DAR project, as he is an expert in sustainable exploitation of groundwater resources with special regard to coastal aquifer management, giuseppe.sappa@uniroma1.it

**19** Giulia Luciani is a PhD student at DICEA – Department of Civil, Building and Environmental Engineering, Sapienza University of Rome, where she graduated in Environmental Engineering. She participated at the activities of ACC-DAR project on a scholarship. Her research interests include assessment of impacts of climate change on water resources, sustainable groundwater management and artificial recharge of groundwater.

Authors thank Silvia Macchi for involving them in this really interesting and attractive experience.

as lithological properties of outcropping geological formations and their main hydro-geological settings, as well as chemical groundwater characterization also depend on them, but they were not the target of the study.

## 6.2 The Study Area

The United Republic of Tanzania is a country in Sub-Saharan Africa. It borders Kenya to the North, Uganda, Rwanda, Burundi and the Democratic Republic of the Congo to the West, and Zambia, Malawi and Mozambique to the South. The city of Dar es Salaam is the largest urban center of Tanzania, with a population of about 3 million people and a growth rate of 4.3%. The region of Dar es Salaam is divided into the three districts of Ilala, Kinonondoni, and Temeke. In the last two decades, the increased demand of water due to growing urbanization and uncontrolled groundwater abstraction due to scarcity of surface water resources has placed the principal coastal aquifer of Dar es Salaam in a growing danger of salinization. The possible presence of various sources of salinity in the area has been documented. These include: seawater intrusion and anthropic contamination due to overexploitation, and water ascending from deep marine sediments (Mjemah 2007). The study area covers a surface area of approximately 260 km<sup>2</sup>. It extends along a 40 km stretch of coastline to the north of the city center, and includes a part of the city center, and some peri-urban areas.



**Figure 6.1:** Study area.

The study area was selected on the basis of hydrogeological boundaries: the eastern boundary is the Indian Ocean, the western boundary is the Dar es Salaam Plateau, which rises west of the ocean along the entire study area up to the Pugu Hills, the southern and northern hydrogeological boundaries are, respectively, the Mzinga River and the Nyakasangwe River (Sappa *et al.* 2013a).

### 6.3 Geological and Hydrogeological Framework

The geological structure of Tanzania reflects the geological history of the whole African Continent. The oldest rock basement in coastal Tanzania includes the Precambrian sediments of the Archean age. The continental Karoo sequence forms the basal part of the sedimentary sequence in the coastal basin of Tanzania. Alternating periods of regression and transgression characterized the Jurassic, Cretaceous and Tertiary (Paleogene and Neogene) ages. In regression periods, clays, silty layers, and silty limestone dominated. In transgression periods, sediments mainly consisted of calcareous, sandy, and shelly limestones. The Neogene period (Miocene and Pliocene) in the study area was characterized by important tectonic activities, which defined the present topographic features.

Neogene sandstone formations, interbedded with siltstones and mudstones, occupy the upland zone south and west of the city center. Within the Neogene formations, several distinct varieties are recognizable. Sandstones occupy over three quarters of the region and comprise a variety of main types. The most important outcrop of the Miocene is the kaolinitic sandstone in the Pugu Hills. The massive terrace sandstone is the bedrock that limits the extent of terraces (Msindai 2002). The Pugu sandstones comprise massive, kaolinitic, and cross-bedded sandstones. Calcareous sandstones also occur on back reef areas of the uplands.

During the Quaternary period, deposition and erosion processes occurred in relation to tectonics, sea level, and climate change. In the coastal region of Dar es Salaam, the quaternary deposits can be divided into three geological layers: alluvial, coastal plain, and coral reef limestone deposits. Alluvial deposits fill the valleys of the Mzinga, Kizinga, and Msimbazi rivers. They consist of an alternation of fine and coarse-grained sands, clay, and sometimes gravel and pebbles. The coastal plain consists of unconsolidated sediments, predominantly sandy, with evidence of several marine intercalations. The presence of coralline limestone is found along the coastal strip. Carbonate rocks are present as fringing reefs and raised reefs. The northern part of the region has few fringing reefs, while raised reefs dominate the western margins of the upland.

The geological setting of the study area comprises unconsolidated sediments of Neogene and Quaternary ages (Figure 6.2). The alluvial deposits and coastal plain deposits are of Pleistocene to Recent age and are found mainly moving from the coast towards the mainland within the river valleys. The main part of the study area cor-



deposits from Pleistocene to the Recent age. The unconfined aquifer consists of fine to medium sand, with varying percentages of silt and clay. Due to the high percentage of sand, it is defined as a sand aquifer, which is considered the most important aquifer for water supply. The lower, semi-confined aquifer consists of medium to coarse sands. The lower aquifer overlies the substratum formed by Mio-Pliocene clay-bound sand and gravel and kaolinitic Pugu sandstones. The different hydrogeological formations characterizing the groundwater system in the area of concern are described in Table 6.1 below (Mjemah 2007).

**Table 6.1:** Hydrogeological scheme.

AQUIFER	PERIOD	EPOCH	LITHOLOGY	THICKNESS (m)
Unconfined	Quaternary	Pleistocene to recent	Fine to medium sand with silts and clay, coral reef limestone and calcareous, alluvial clay, silts and gravels	5–50
Aquitard	Quaternary	Pleistocene to recent	Clay, sandy clay	10–50
Semiconfined Aquifer	Quaternary	Pleistocene to recent	Medium to coarse sand and gravels with clay	100
Aquitard	Neogene	Mio-Pliocene	Clay-bound sands	≈ 1000

## 6.4 Methodology

The current state of groundwater quality in the coastal aquifer of Dar es Salaam was studied through the implementation of various methods, tailored to the available set of climatic and hydrogeological data (both historical and current data).

A review of available literature was conducted to assess the geological and hydrogeological sketch framework of the Dar es Salaam coastal plain. Climatic and anthropogenic influences on hydrogeological dynamics were investigated through the analysis of temporal evolutions of the groundwater recharge. Seawater intrusion was evaluated by hydrochemical methods, through physical and chemical testing of a monitored network of representative boreholes.

## 6.5 Data Collection and Analysis

Two main activities were carried out: collection of historical data from a variety of existing sources, and the execution of two groundwater monitoring campaigns in June and November 2012.

The output of these activities is a set of historical data that includes the climatic parameters precipitation and temperature data for 3 gauges with reference to the last 50 years, hydrogeological characteristics of the coastal aquifer, and the physical and chemical parameters of the groundwater for nearly 400 boreholes located in the Dar es Salaam region. These data have been collected and organized in a database, ACC-Dar Borehole Monitoring Database ([http://www.planning4adaptation.eu/042\\_Maps.aspx](http://www.planning4adaptation.eu/042_Maps.aspx)).

A subset of boreholes located in the study area was chosen for the monitoring network from the database of 400 georeferenced boreholes, with consideration for uniformity of spatial distribution: the network consists of 79 boreholes, uniformly distributed with a frequency of about 1 borehole per 3 km<sup>2</sup>. The study area and the borehole monitoring network are shown in Figure 6.3. The boreholes concerned with a monitoring campaign are commonly used to satisfy civil private demand. For many of them depth is unknown, and as they are all equipped with a pump, the collected samples can't be referenced to a specific depth, therefore they are representative of the average thickness of the aquifer crossed through.

## 6.6 Climate Change Effects on Active Groundwater Recharge

Hereinafter are presented elaborations and results regarding evaluation of contribution to Average Annual Groundwater Recharge (AAGR) coming from direct infiltration in the area under study. Although the values discussed may only be part of the total active groundwater recharge of the area, this is the majority of it, and so, this aspect should not affect the conclusions drawn.

AAGR was evaluated using the Hydrogeological Inversed Budget Method (Civita and De Maio 1999) as modified by Sappa, Trotta, and Vitale (Sappa *et al.* 2014). This method involves a spread parameters approach, based on the discretization of the study area in cells, and for each cell the estimation of climatic, topographical and hydrological input parameters usually available and involved in the evaluation of the hydrogeological budget.

The values of Average Annual Precipitation (AAP), to be assigned to each cell, were determined from the Annual Average Precipitation values, and recorded in the gauging stations through appropriate techniques of spatial interpolation. Due to the absence of temperature values necessary for the calculation of evapotranspiration, as well as the land cover properties, the application of the method was performed, as suggested by the authors, enclosing the effects of evapotranspiration and runoff, directly in the potential infiltration factor (PIF). This coefficient represents the amount of rainfall reaching the subsoil and contributing to groundwater recharge, ranging between 0 and 0.55, depending on land cover characterization. The values of Average Annual Infiltration (AAI), given to each cell and expressed in mm, are calculated as a product of the PIF and the AAP. The correspondent average annual volumes infil-

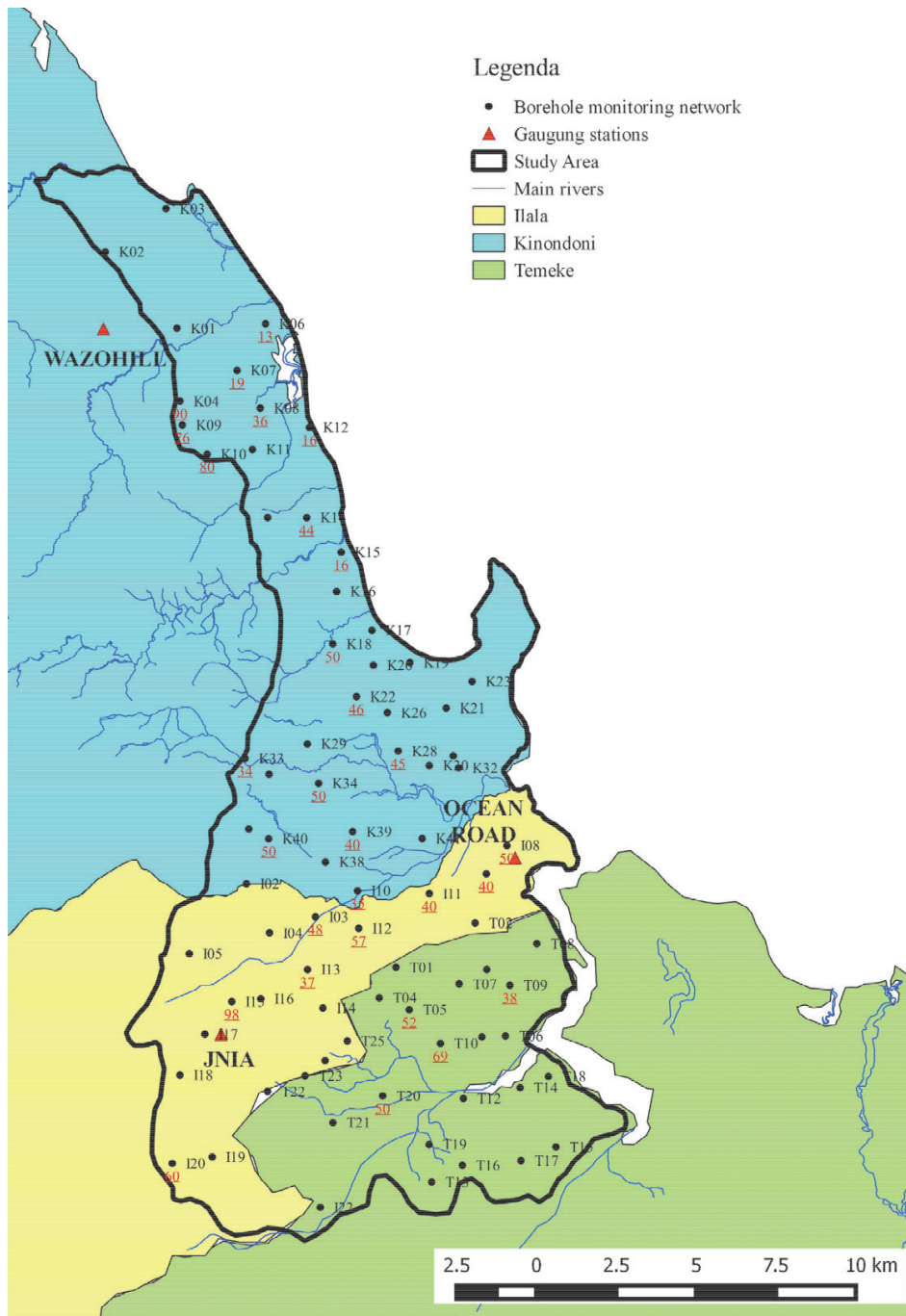


**Figure 6.3:** The study area and the monitoring network in 2012. Where known, the depth of the boreholes is indicated.

trated are obtained as a product of the AAI and each cell area. Finally, the amount of AAGR, referred to the whole study area is obtained by the addition of values assigned to each cell.

The study area was divided in 500m x 500m squared meshes. Precipitation records for the previous 50 years, from 1960 to 2010, were collected in 3 meteorological stations in Dar es Salaam: JNIA, Wazohill, and Ocean stations.

Since only the JNIA station, located close to the international airport of Dar, had data for every one of the 50 years, statistical elaboration processes were applied in order to create the missing data for the other stations. To determine these data, three different methods were used: (i) between-station, method based on the average of the data registered in adjacent different stations; (ii) within-station method, based on the average of the earlier and later data; and (iii) regression following the WMO approach (WMO 2011), which is based on an important result: as concurrent values of rainfall in relation to two stations are compared, their difference (temperature) or their ratio (precipitation, wind speed) tends to be constant.

Afterwards, as the missing data series were recreated, data's adaptation to theoretical distributions through the method of moments was verified. Two different statistical tests, Pearson and Kolgomorov Smirnof, were conducted. Only the Gaussian distribution passed both tests.

For each station, referring to the Gaussian distribution, the rain values, which define the range corresponding to a 68% of probability of occurrence, defined by the mean ( $\mu$ ) and the std.dev ( $\sigma$ ) as  $(\mu-\sigma)$  and  $(\mu+\sigma)$ , were chosen as representative of the minimum and maximum probable rain value for the station. These values were used for successive elaborations and are shown in Table 6.2.

**Table 6.2:** Average Annual Precipitation (AAP) values for the three meteorological stations (1960–2012).

Jnia	$\mu+\sigma$	1410 mm
	$\mu-\sigma$	854 mm
Ocean Road	$\mu+\sigma$	1249 mm
	$\mu-\sigma$	801 mm
Wazo Hill	$\mu+\sigma$	1091 mm
	$\mu-\sigma$	727 mm

In order to spread these values over the study area, the Inverse Distance Weighting method (IDW) was used, which is deterministic for multivariate interpolation. The IDW method was applied three times to determine the minimum, mean and maximum of rain values for each station, respectively.

In the present study, the values of PIF were assigned to each cell on the basis of land cover interpretation data, coming from elaboration of the analysis of satellite images (Congedo *et al.* 2013), carried on by another research team involved in the same ACC-DAR project. The interpretation of these data permitted assessment of the evolution of land cover in the study area for a period of ten years (2002–2012), and allowed us to associate PIF values to the different land cover properties outcropping in the study area, as it is reported in Table 6.3.



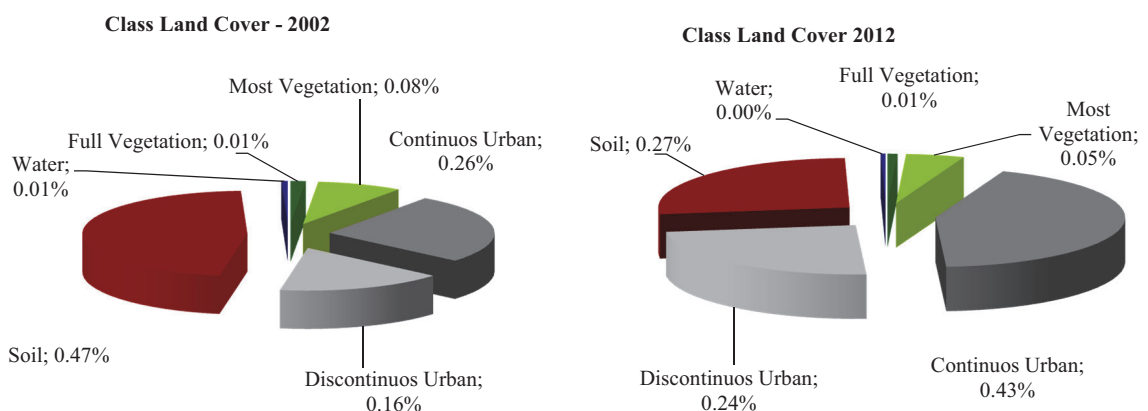
**Table 6.3:** Potential Infiltration Factor (PIF) values, given to the different land cover class.

Land cover	PIF
Out of city	0,15
Unclassified	0,15
Full vegetation	0,3
Mostly vegetation	0,4
Continuos urban	0,1
Discontinuos urban	0,2
Soil	0,3
Water	0,55

Data on land cover evolution in Dar Es Salaam (Congedo *et al.* 2013) were elaborated, and for each year a PIF value was given to each 500m x 500m square cell.

During the 2002–2012 period, an impactful demographic growth occurred, involving substantial changes in urbanization and land cover. The analysis of land cover evolution between 2002 and 2012 shows that urban land, as both continuous urban and discontinuous urban land, increased from 40% to 65%, following a linear trend. Meanwhile, over the last 10 years, soil, which is the land cover type with the maximum PIF value, decreased by 20%, from about 47% to about 27%. The increase in urban areas transformed the region, rendering it less permeable to rainfall. As a result, many areas are now contributing less to the recharging process than before (Sappa *et al.* 2013a).

A range of possible values of AAGR for the study area was estimated. The estimate was made considering the land cover of 2011 and the AAP values calculated on the basis of the 52-year data set. AAP values are expressed in terms of minimum, medium

**Figure 6.4:** Percentage variations of land cover distribution (2002–2012)

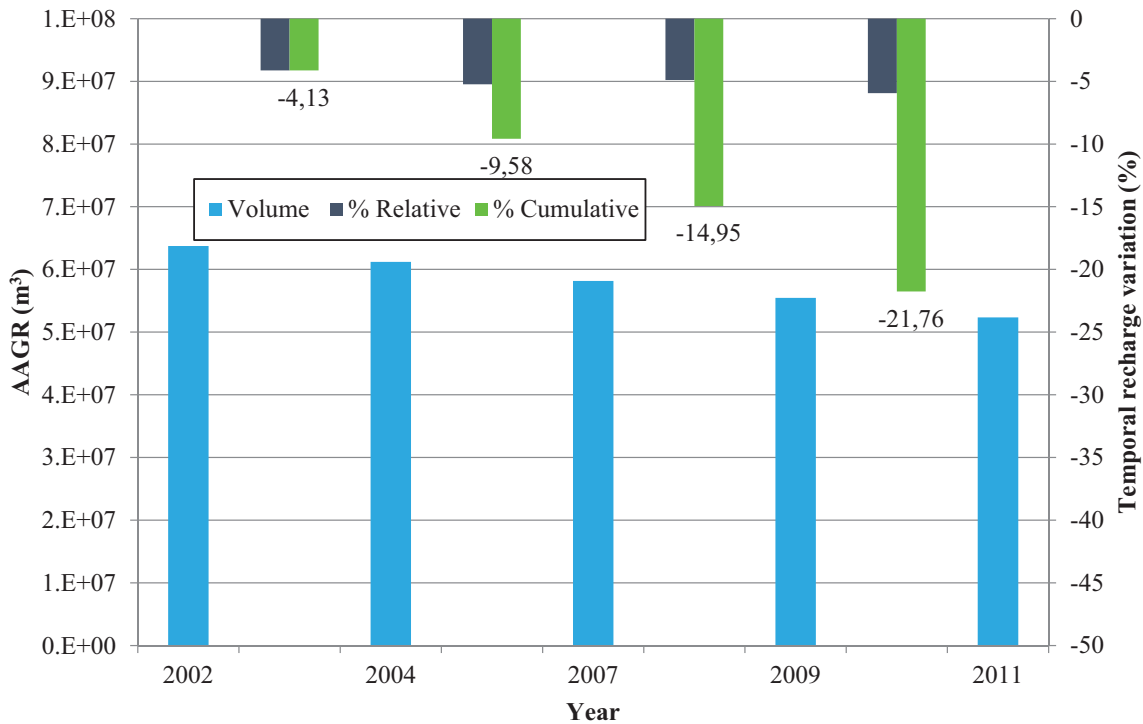


**Figure 6.5:** Average Annual Groundwater Recharge (AAGR) temporal variation in the period 2002–2011.

and maximum values, which correspond to the 0.7 decile result of the Gaussian distribution for the AAP data set. Land cover for the year 2011 was 29% soil, 65% urban, and 6% vegetation. The estimated corresponding volumes of infiltration (AAGR) are  $4.0 \times 10^7$ ,  $5.2 \times 10^7$  and  $6.4 \times 10^7$  m<sup>3</sup>, respectively. Values obtained were compared with similar results coming from previous studies, and they seemed very similar (Van Camp *et al.* 2012).

The evolution of AAGR in the period from 2002 to 2011 was analyzed, considering the AAP and land cover of each year. The analysis showed a decrease of 20% in AAGR from 2002 to 2011, almost 5% for each year.

As a further investigation, analysis of the rainfall evolution (mm) in the last decade for the study area was carried out. It was determined that, although the AAP decreased over the last decade for all of the monitored stations (Figure 6.6a), the changes in precipitation amount were only slight in the last five years (Figure 6.6b), and AAP appears to be almost the same, with values between 900 and 1000 mm/y. Thus, in recent years most of the decreases in groundwater active recharge likely originated from land cover use modifications.

Based on the results of the previous recharge estimate, a prediction was made of estimated AAGR volumes from 2013 to 2020, assuming a constant rate of precipitation (the analysis was carried out using the mean estimated values for each station) and assuming a linear trend of urban land cover increasing.

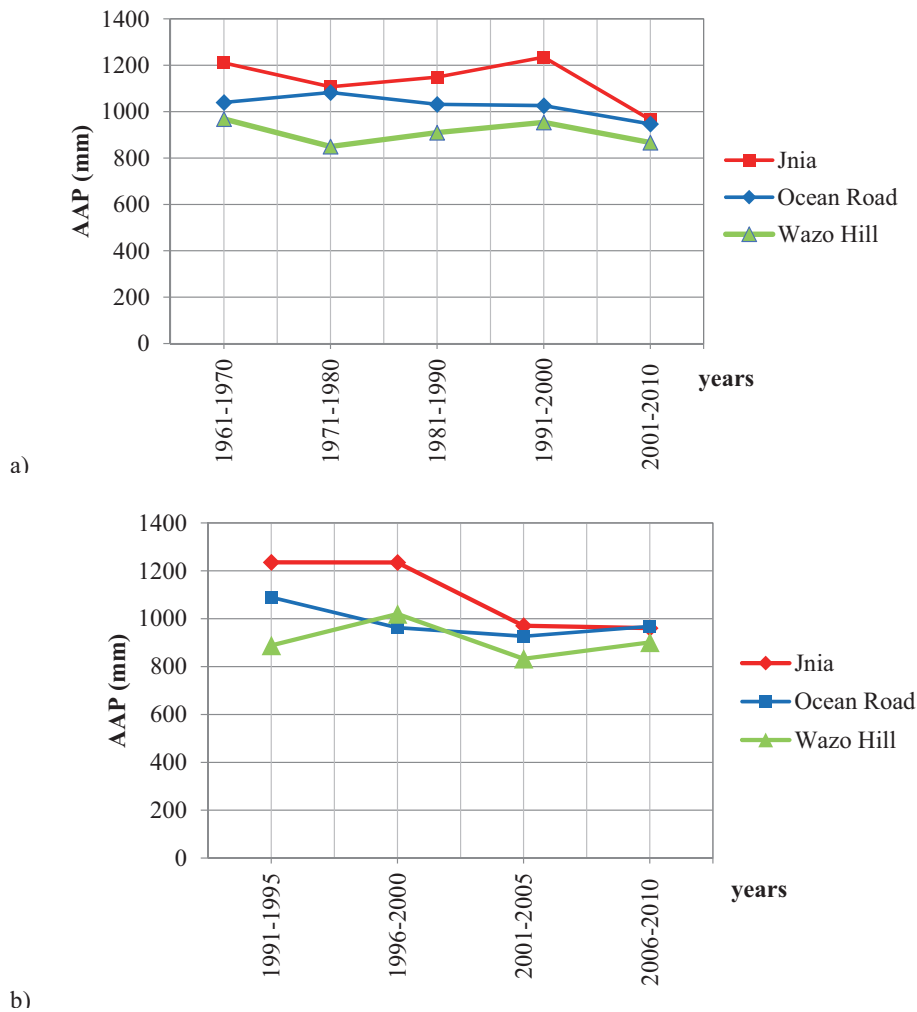


**Figure 6.6:** a) and b) Average Annual Precipitation (AAP) referred to any 10 and any 5 years.

In the diagram of Figure 6.7, the AAGR, calculated for the last decade, and the linear regression line relating to these values was drawn. From this interpolation, the corresponding evolution of AAGR from 2012 up to 2020 was extrapolated. For 2020, a recharge value of  $5.0 \times 10^7 \text{ m}^3$  was estimated, representing a 14% decrease in AAGR across the timeframe considered, 2012–2020 (Sappa and Ioanni 2013b).

## 6.7 Seawater Intrusion Assessment

The main parameters that indicate the groundwater salinization rate are electrical conductivity (EC) and chloride (Cl<sup>-</sup>) concentration. EC depends on total salt concentration, which is the major quality factor generally limiting the use of saline waters for crop production. FAO (Rohades 1992) and WHO (2003) guidelines indicate that waters with EC values higher than 2000 and 1500  $\mu\text{S}/\text{cm}$ , respectively, are not suitable for drinking or for irrigation. Results of the chemical analysis of groundwater in June 2012 (79 samples), showed that 25.3% of the samples were not suitable for drinking

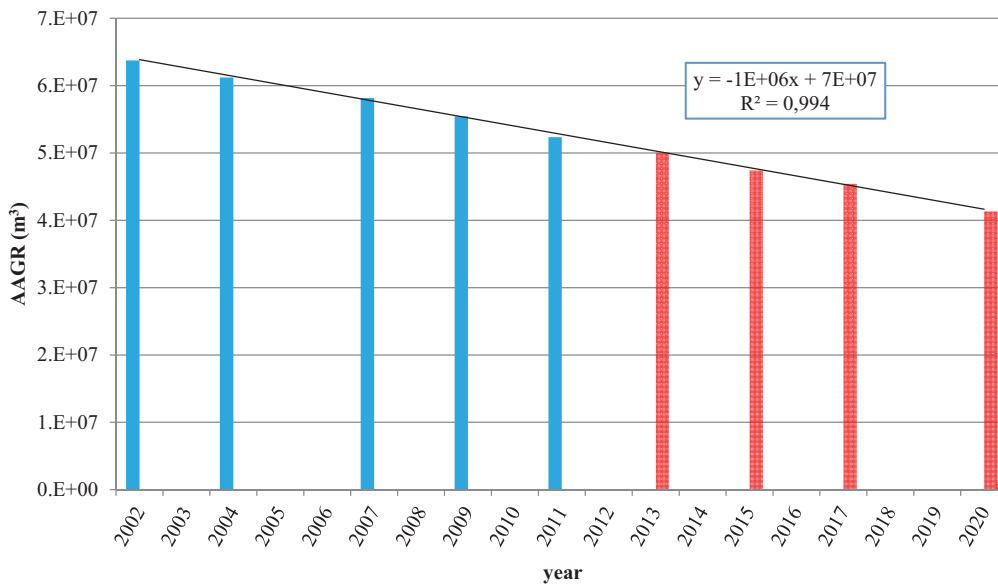


**Figure 6.7:** Estimate of temporal evolution of AAGR (m<sup>3</sup>) from 2012 to 2020.

or irrigation according to FAO guidelines for EC (36.7% according to the WHO classification).

The analysis of the temporal evolution of EC and chloride concentration in groundwater, in the period 2002–2012, is useful to assess the presence of seawater intrusion. In coastal aquifers an increase of EC can be attributed to different factors, such as seawater intrusion, the processes of dissolution of carbonate, the presence of anthropogenic pollutants, (i.e. nitrates, phosphates, sulphates) coming from civil activities or those related to agricultural and industrial sectors, and in some cases, by fossil saline water rising from the deeper layers of the aquifer. To assess whether increases in EC are related to seawater evolution, the parallel increase of chloride concentrations in groundwater were analyzed. Chloride is the most abundant ion in seawater (seawater contains approximately 35,000 mg/l of dissolved solids, which include about 19,000 mg/l of chloride, while fresh-water generally contains less than 30 mg/l). Moreover, chloride is chemically stable, as it is not involved in ionic exchange processes, and thus moves at about the same rate as intruding seawater. Therefore, an increased chloride concentration in a freshwater aquifer is the most commonly used chemical indicator of seawater mixing with freshwater. The analysis of the evolution of chemical composition of groundwater was carried out for boreholes where measures from different years were available in the period 2001–2012. The total number of wells available for this type of processing was 15, 10 of which were in the Kinondoni area, 2 in Ilala, 3 in Temeke.

Boreholes with the highest percentage increases in EC also had the highest percentage increases in chloride content. Boreholes K08 and K14, which are in the northern coastal area of Kinondoni, in the wards of Kunduchi and Kawe, respectively, showed the greatest percentage increase in EC. These areas also had high percent-

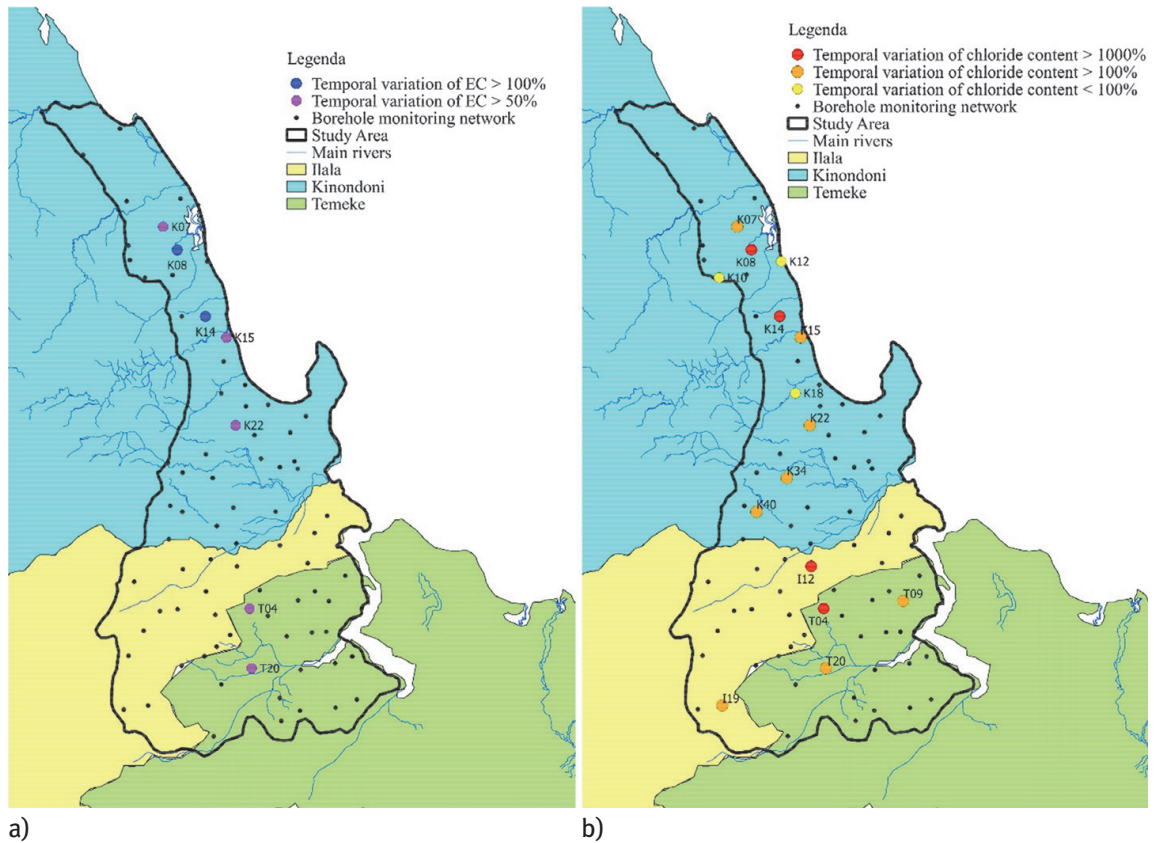


**Figure 6.8:** Temporal evolution of EC (a) and chloride content (b) of groundwater in the period 2003–2012.

age variations in chloride content in groundwater, with slightly higher values in K22 (Mikocheni), K34 (Sinza) and in K40 (Mabibo). Other areas with high increases of chloride content were in the wards of Buguruni in Ilala (I12) and Chang’hombe in Temeke (T04). Moreover, areas affected by sensitive increases of chloride concentrations in groundwater are, from the north to the south, Miburani (T09), Yombo Vituka (T20) and Kitunda (I19).

In order to verify results from the previous analysis, the following diagrams were created. They show the comparison between ions mainly of marine origin ( $\text{Cl} + \text{SO}_4$ ) and ions mainly of continental origin ( $\text{Ca} + \text{Mg}$ ), expressed in milliequivalents, obtained from boreholes during in the period 2001–2012, as these were the available measurements relating to more than one year. In the following diagrams, the evolution of ( $\text{Ca} + \text{Mg}$ ) and ( $\text{Cl} + \text{SO}_4$ ) content in the boreholes is described. The larger symbols represent more recent data. All the graphs, particularly those referring to the area of Kinondoni, currently show higher concentrations of marine ions than those observed in the previous decade.

On the other hand, groundwater recharge mainly occurs during the long rainy season (March to May) and to a lesser extent during the short rainy season, i.e. between October and December, as shown by the analysis of average monthly values of precipitation registered at JNIA station during the last 50 years, which is represented in

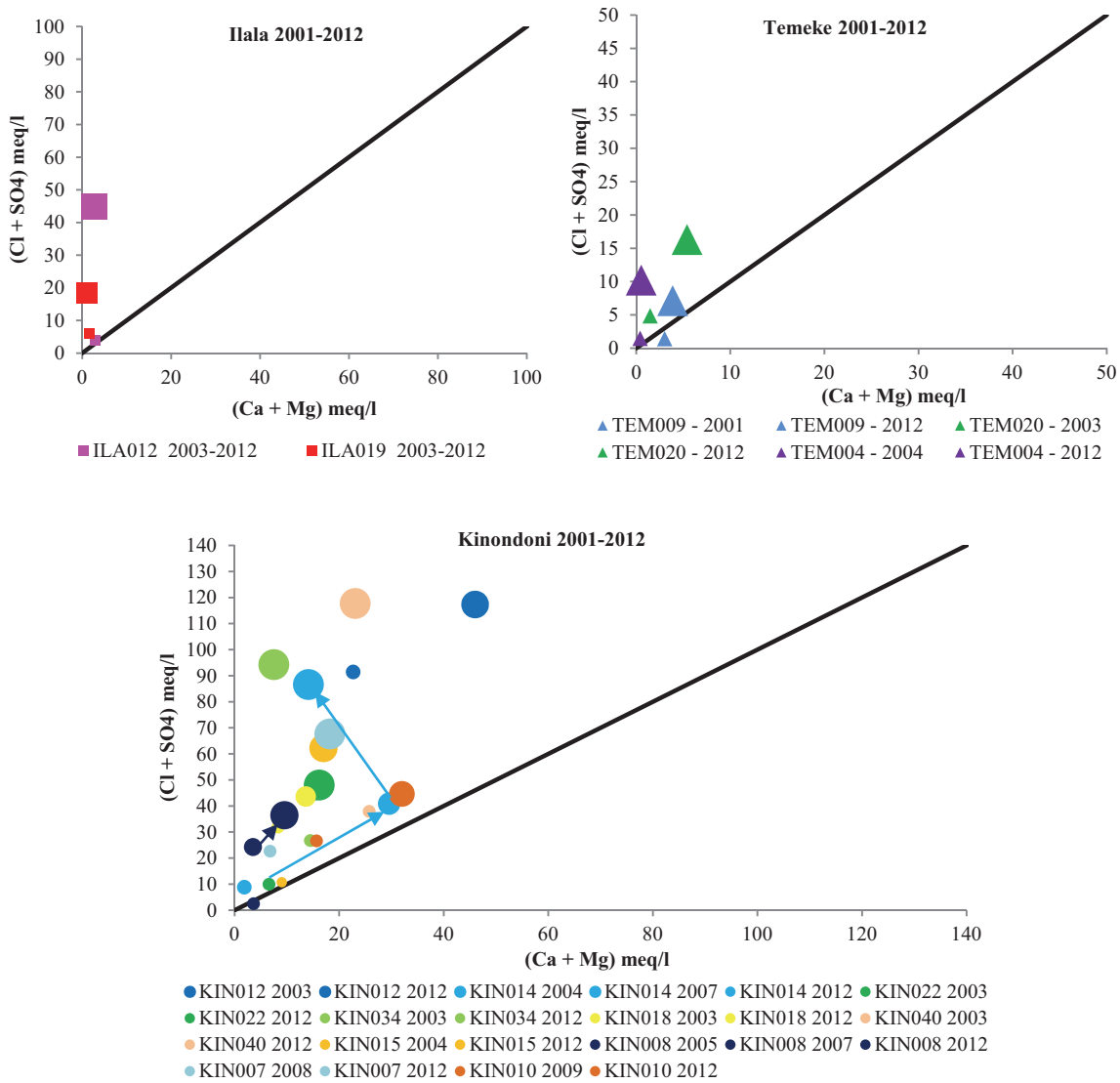


**Figure 6.9:** Diagram of (Ca+Mg) vs. (Cl+SO<sub>4</sub>) for the three districts for the period 2003–2012.

Figure 6.11. Recharge during the long rainy season accounts for about 85% of the total annual recharge, with an important peak in April, whereas recharge occurring during the short rainy season contributes to only 15% of the total annual recharge, with a small peak in November (Mtoni *et al.* 2012).

Based on monitoring done in June and November 2012, a geochemical analysis enabled the identification of some features and some seasonal variations of groundwater chemistry, which are a possible indicator of the presence of various processes underway in the area. Chemical analysis were carried out on 79 samples collected in June 2012 (representing the end of the main wet season) and on 71 samples collected in November 2012 (representing the peak of the minor wet season). The interpretation was based on statistical parameters of principal ions present in groundwater, water type classification according to Stuyfzand classification system (1989) and scatter diagrams of principal ions.

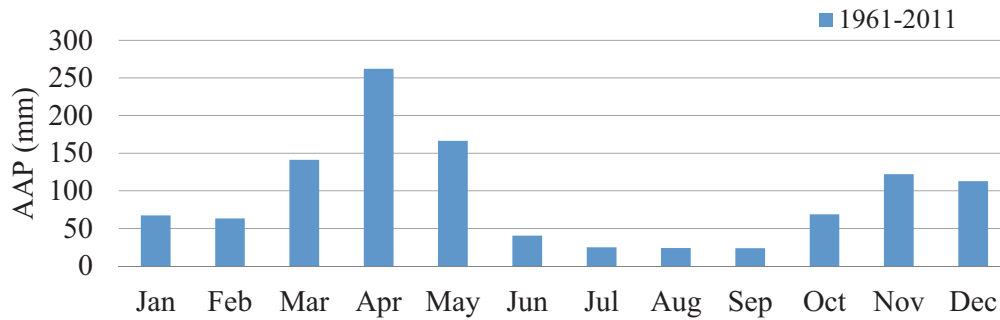


Figure 6.10: Average monthly rainfall for Dar es Salaam.

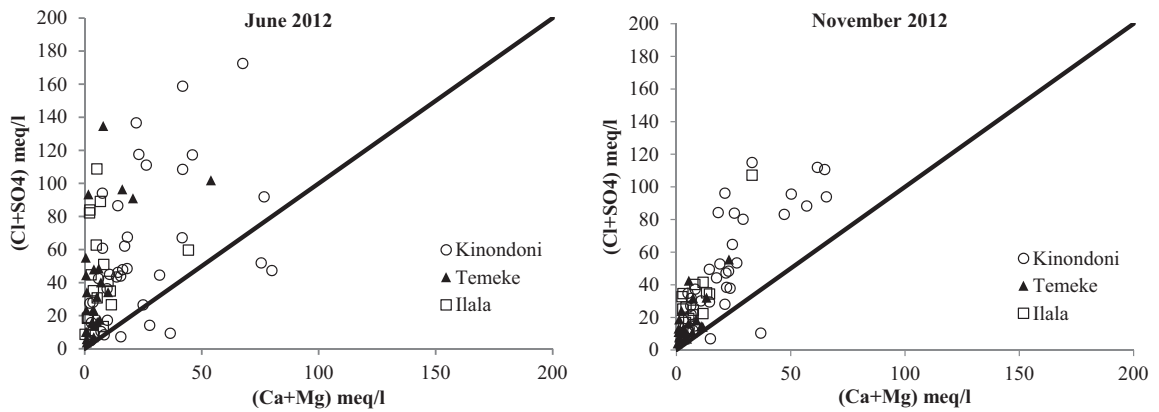
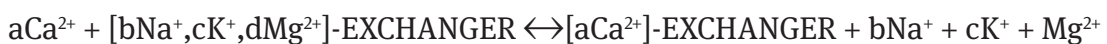


Figure 6.11: Diagram of (Ca+Mg) vs. (Cl+SO<sub>4</sub>)

Stuyfzand classification subdivides water types in four steps, including chloride content, alkalinity, dominant ions and the parameter Base Exchange Index (BEX) (Stuyfzand 1989), which is:

$$BEX = (Na+K+Mg)_{corrected} = (Na+K+Mg)_{measured} - 1,061Cl \text{ (meq/l)}$$

This parameter represents the difference between principal marine cations, which are found in the sample, and the expected values of these for seawater. Seawater intrusion leads to negative values of the BEX index (i.e. samples of class 1, according to the classification represented in Table 6.4). The definition of the BEX index is based on the description of the ionic exchange process that occurs when seawater intrudes in a fresh-water aquifer, which is described by the following reaction, where a,b,c,d represent molecular concentrations, with the balance in milliequivalents:  $2a = b+c+2d$ :



In the early stages of seawater intrusion, an ion exchange process generally takes place. As such, when salt water intrudes an aquifer containing fresh water, sodium replaces calcium on the aquifer’s clay particles through ion exchange before significant chloride increases are observed. This involves a decrease in Na<sup>+</sup> concentration

**Table 6.4:** Stuyfzand classification.

Stuyfzand classification			
Main type	Cl <sup>-</sup> (mg/l)	< 5	very oligohaline (G)
		5–30	oligohaline (g)
		30–150	fresh (F)
		150–300	fresh-brackish (f)
		300–1000	brackish (B)
		1000–10000	brackish-salt (b)
		10000–20000	salt (S)
		> 20000	hyperhaline (H)
Type	Alk (meq/l)	< 1/2	very low (*)
		1/2–1	low (0)
		1–2	moderately low (1)
		2–4	moderate (2)
		4–8	moderately high (3)
		8–16	high (4)
		16–32	very high (5)
		32–64	extremely high (6)
		64–128	extremely high (7)
		128–256	extremely high (8)
> 256	extremely high (9)		
$(\text{Na}+\text{K}+\text{Mg})_{\text{CORRECTED}}$ (meq/l)		Class	
$(\text{Na}+\text{K}+\text{Mg})_{\text{CORR}} < \sqrt{0,5}\text{Cl}$ and $(\text{Na}+\text{K}+\text{Mg})_{\text{CORR}} < 1,5(\Sigma\text{cat} - \Sigma\text{an})$		1	
$\Sigma\text{cat} = \Sigma\text{an}$ and $ (\text{Na}+\text{K}+\text{Mg})_{\text{CORR}} + (\sqrt{0,5}\text{Cl})^*(\Sigma\text{cat} - \Sigma\text{an})/ \Sigma\text{cat} - \Sigma\text{an}   > 1,5(\Sigma\text{cat} - \Sigma\text{an})$		2	
$(\text{Na}+\text{K}+\text{Mg})_{\text{CORR}} > \sqrt{0,5}\text{Cl}$ and $(\text{Na}+\text{K}+\text{Mg})_{\text{CORR}} > 1,5(\Sigma\text{cat} - \Sigma\text{an})$		3	

in groundwater, and a parallel increase in  $\text{Ca}^{2+}$ . Conversely, when seawater is flushed by freshwater, most abundant ions in freshwater such as  $\text{Ca}^{2+}$  expel and replace the  $\text{Na}^+$ , absorbed in the solid matrix, and sodium is released into the water. Therefore a decrease in the molar ratio of sodium to chloride can be used as an indicator of seawater intrusion, while an increase in the ratio can be used as an indicator of flushing of the aquifer by freshwater (Stuyfzand 1992, Walraevens 2004).

Scatter diagrams  $(\text{Ca}+\text{Mg})$  vs.  $(\text{Cl}+\text{SO}_4)$  allow the comparison between relative concentrations of typical marine origin ions and typical continental ions. In samples



from both months of investigation, Cl and SO<sub>4</sub> ion content prevails over (Ca+Mg) content. This is a possible indicator of the presence of seawater. For boreholes of Ilala and Temeke, a predominance of marine ions is clearly indicated, while samples coming from Kinondoni boreholes appear dispersed and show high a content of Ca and Mg. The presence of water with these prevailing ions could be due to carbonate dissolution, related to calcareous formations outcropping, and ionic exchange processes. The boreholes of known depth, which show the higher concentrations of marine ions are K33, K39, K40, K34, T10, K12, K14, I13 and I15 in June, and K09, K06, K04, K33, K39, K40 and K14 in November.

Some of the ionic ratios are characteristic of the water types. As seawater is rich in Cl<sup>-</sup> ions (chloride) and continental waters are rich in HCO<sub>3</sub><sup>-</sup> (bicarbonate), a diagram of Cl vs. Cl/HCO<sub>3</sub> is used to evaluate the level of salinization. The values of the Cl/HCO<sub>3</sub> ratio given for fresh water are between 0.1 and 5, and for seawater between 200 and 500 (Custodio 1987). In the diagrams of Figure 6.12, the lower line represents a typical value of the Cl/HCO<sub>3</sub> ratio expected for fresh waters, which is 0.5 (Al Farrah and Walraevens 2011, Mtoni 2013). When fresh waters exhibit ratio values exceeding this, they have to be considered as being affected by salinization. The line at 6.6 represents a typical value indicating highly salinized waters (Al Farrah and Walraevens 2011, Mtoni 2013). Analysis of Cl vs. Cl/HCO<sub>3</sub> diagram (Figure 6.12) shows that samples from both months of investigation are all affected by salinization. Considering boreholes of a known depth, as in June and November 2012, the most salinized samples presenting with higher chloride concentrations are borehole KIN033, KIN034, KIN039, KIN040, all located in the center of the study area, and KIN006 and KIN014 in the northern coastal zone in Kinondoni. On the contrary, boreholes ILA013, ILA015 and KIN012 exhibit high salinization from the June investigation only, while boreholes KIN004 and KIN009 show high salinization only in November.

Other samples with high salinization, but with a lower content of chlorides are those from boreholes I03, I08, I09, I10, I11, I12, I20, in the SW of the study area

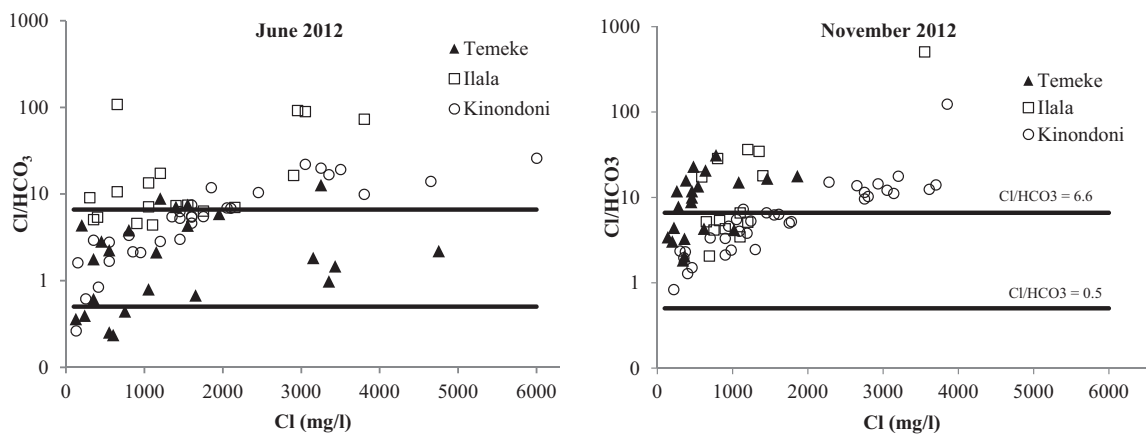
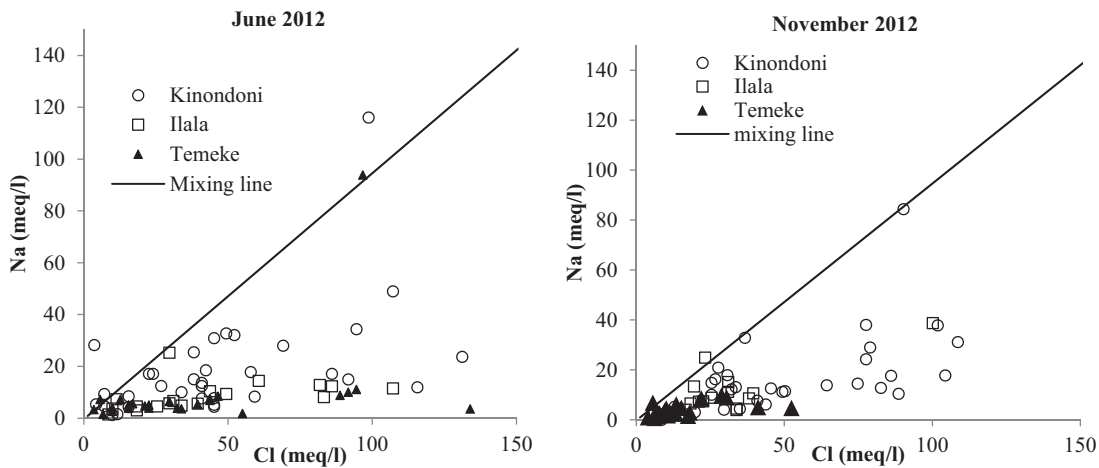


Figure 6.12: Diagram of Cl<sup>-</sup> vs. (Cl<sup>-</sup>/HCO<sub>3</sub><sup>-</sup>)



**Figure 6.13:** Diagram of  $\text{Cl}^-$  vs.  $\text{Na}^+$

(respectively in wards of Tabata, Upanga West, Jangwani, Mabibo, Mchikichini, Buguruni and Yombo Vituka), and boreholes K07, K10 (wards of Kunduchi in the northern coastal area of Kinonondoni), K15 and K22.

In June, for boreholes in the northern coastal area of Kinondoni a possible trend in salinization can be identified, as salinization increases going toward the north, along the coastal strip: between the two lines in the diagram, from the bottom upward, with some exceptions, boreholes K23, K28, K17, K04, which are localized in an orderly way from the south to the north along the coastal strip, follow a growing trend of salinization. In June boreholes of Temeke present the minor salinization and chloride content. For these boreholes, low values of  $\text{Cl}/\text{HCO}_3$  are due to high concentrations of  $\text{HCO}_3$  ions. Borehole T10 exhibits high concentrations for all ions, which could be ascribed to associated anthropogenic contamination. In November all boreholes are affected by salinization.

As chloride can be considered like a conservative tracer, because it is not involved in the ionic exchange processes, it is representative of the proportion of seawater intruding into the aquifer. The analysis of graphic relationships between  $\text{Cl}^-$  and the other major ions, like Ca and Na, relative to the simple mixing lines, is useful in identifying additional processes, such as ionic exchange, annexed to the mixing phenomenon. A simple mixing line can be drawn in the diagrams, starting from the known composition of two extremes, freshwater and seawater. These dilution lines represent the theoretical gradual (linear) transition from one water-type to the other that occurs in the transition zones in coastal aquifers. If samples follow the dilution lines, the source of the plotted ions is fresh groundwater mixed with the seawater. The mixing lines that appear in the diagrams were constructed by the two extremes of freshwater and seawater collected in October 2013. The concentrations of major constituents present in the sampled waters were compared with corresponding values of dilution lines. In diagram of Cl vs. Na (Figure 6.13), almost all samples are under the dilution line, meaning that sodium concentrations are lower than the expected quantities in

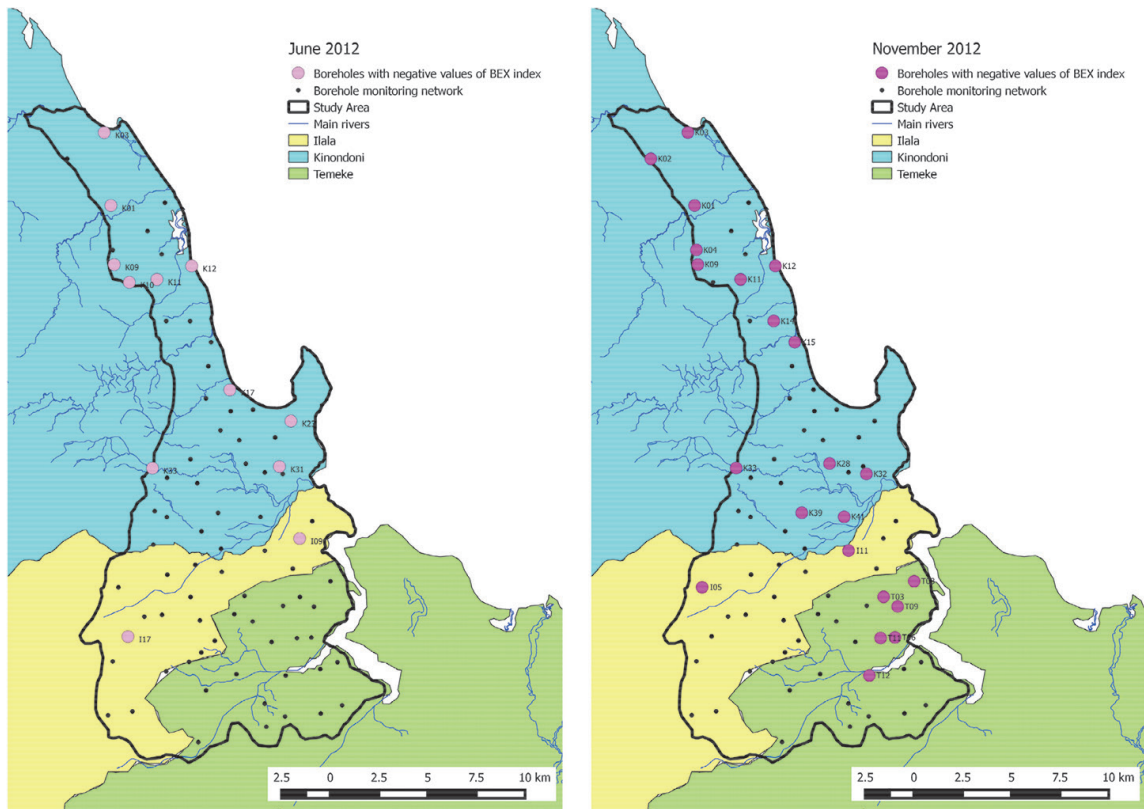


**Figure 6.14:** Boreholes with negative values of BEX index in June and November.

the presence of simple mixing with marine waters. This result is a possible indicator of the process of ionic exchange associated with seawater intrusion. For both months of investigation, samples from Kinondoni appear scattered, while the same samples of Ilala and Temeke seem more grouped along defined directions. It can be distinguished from the group corresponding to boreholes of the central area (K33, K34, K39, K40, with I13, I15 and T10), which presents sensitive deviations from dilution line. For the other samples, from boreholes for the most part from Ilala and Temeke and the rest of boreholes referred to Kinondoni, chloride concentrations are lower, but regardless they present deviations from the dilution line, indicating the presence of ionic exchange associated with seawater intrusion, and thus suggesting simple dilution of seawater into freshwater.

Concerning the Stuyfzand classification, analytical results show a slightly different distribution of samples in various classes for the two months of investigation. A decrease in samples classified as brackish-salt (72.7% in June and 60% in November) can be seen in November, but also a major number of samples with negative values of BEX index (21% in June, 33.3% in November), signifying an increase in the number of boreholes with signals of seawater intrusion (Sappa *et al.* 2013c). This occurs in many boreholes in Temeke's districts in particular, and in some boreholes of the southern districts of Kinondoni, in the centre of the study area.

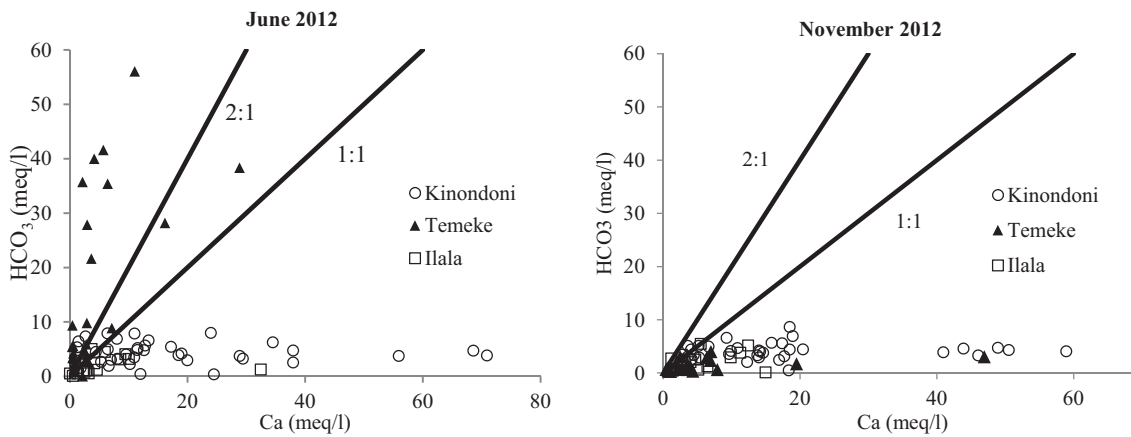
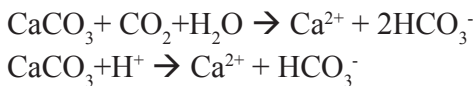


**Figure 6.15:** Diagram of  $\text{Ca}^{2+}$  vs.  $\text{HCO}_3^-$

The quaternary deposits, underlying the coastal plain of Dar es Salaam also include coral reef limestone near the coast. Calcareous sandstones also occur on back reef areas of the uplands. Dissolution of carbonates releases calcium and bicarbonate into the groundwater; this process can be added to the other factors, determining a TDS increasing. Scatter diagrams of Ca vs.  $\text{HCO}_3^-$  (Figure 6.15) have been used to show the influence of these processes on the chemistry of groundwater in the study area in both months. Lines in the diagram represent the relationship between  $\text{HCO}_3^-$  and  $\text{Ca}^{2+}$  corresponding to the following reaction:



The first one is the typical dissolution reaction of calcite by  $\text{CO}_2$  in the unsaturated zone; the second one represents calcite dissolution by other acids apart from  $\text{CO}_2$ , such as humic acids and protons released from cation exchange (Mtoni *et al.* 2013). In the month of June, it can be seen that a first group of points is arranged according to a slope of less than 1:1, while a second group to a slope greater than 2:1. The first case represents samples from boreholes of Kinondoni, and indicates the presence of an additional process, which add up to dissolution of carbonates. This fact agrees with previous observation about depletion in Na, thus an excess of Ca can be explained as a consequence of both the dissolution of carbonates and the ionic exchange process associated with seawater intrusion. Boreholes of known depth, which present the highest values of Ca and Mg, are K04, K09, K10, K12, K33 and K39. The second group of samples aligns to a slope greater than 2:1, showing enrichment of groundwater in  $\text{HCO}_3^-$ . High values of  $\text{HCO}_3^-$  from samples collected in the month of June can be explained as a consequence of the dissolution of carbonates associated with the meteoric recharge. The depth of most of these boreholes is unknown (K<sub>2</sub>0, T07, T08, T09, T15, T23). Some boreholes of Ilala and Temeke with low concentrations of calcium, follow the dissolution lines.

## 6.8 Conclusions

The present study shows that AAGR has decreased over the past decade due to the combined effects of climate changes and anthropogenic causes. Although recent IPCC assessment reports have concluded that very little is known about the relationship between groundwater and CC (IPCC 2001, 2007, 2008), it is recognized however that CC usually acts as an effects multiplier in already altered hydrogeological systems. The impacts of CC generally lead to a decrease in groundwater quantity and quality. The changes in climatic conditions, which involve significant trends of rainfall decrease, from about 1200mm/year in the 1960s to about 1000mm/year in 2012, and mean temperature increases, have contributed to the decrease of local freshwater resources and an additional demand of groundwater (Sappa *et al.* 2014). Growing urbanization, socioeconomic development and growth of wellness and hygienic demands in cities of semi-arid areas can be considered as an indirect consequence of climate change. In fact, mean temperature rise and rainfall pattern changes due to CC, as agreed by most international climate studies' agencies, are major causes of degradation and unproductivity of cultivated land, and thus causes of abandonment of rural areas by populations, which relocate to big cities, increasing their social stresses and environmental impacts.

Regarding the anthropogenic causes of the AAGR decrease, they can be recognized as both fresh-water resources consumption growth and land cover changes. It has been possible to quantify the changes in land use, occurring in the period 2002–2012. These resulted in an increase of urban areas (from 40% to 65%) and a decrease of soil and vegetation areas (from 55% to 32%), which then considerably reduced the extent of potential infiltration areas.

The analysis of historical chemical data on groundwater composition provided a clear indication of the enlargement of the areas affected by salinization in the period 2001–2012. The origin of this salinization is difficult to determine because it depends on several factors, but the geochemical analysis performed allows us to highlight that a significant contribution to this phenomenon comes from seawater intrusion.

Geochemical analysis showed that chemical composition of groundwater of the most important aquifer of Dar es Salaam is influenced by the seasonal alternation of rainy periods, during which freshwater recharge occurs, and dry seasons, during which evaporation and excessive withdrawals for private water supply increased the degree of salinization of the aquifer. Anthropogenic pressure on groundwater resources follows the cyclical alternation of seasons and emphasizes seasonality effects. In fact, in the dry season, when most of the streams and canals that make up the surface water resources have low flow rates and soil has depleted its moisture content, the population has a greater need to use groundwater reserves to survive and sustain agriculture, and this results in a widespread and huge aquifer overexploitation.

Differences in groundwater chemistry in different areas could be due to both aquifer litology and land cover. Coral reef limestones are present in different loca-

tions along the coastal area. In Kinondoni, where calcareous rocks are found, most groundwater, in both seasons, contain calcium and magnesium.

Regarding land cover influence on different responses to seasonal weather patterns, it can be observed that in Kinondoni, which is the most populated amongst the districts and comprises residential areas provided with hygiene and social services, groundwater overexploitation and consequently salinization lasts all year. The same explanation probably can be applied in the area near to the city center, where the most salinized boreholes are found (K33, K39, K40, I13, I15). Moreover, these areas showed the biggest increase in EC and chloride content in the period 2001–2012. Conversely, in Temeke there are middle to low-income suburbs, characterized by poor settlement planning, low quality housing and social services, and areas used for urban agriculture. As such, urban land cover is less dense, and the effects of natural seasonal weather patterns on groundwater recharge are more evident, with the alternation of salinized and non-salinized composition, as highlighted by scatter diagrams of  $\text{Cl}/\text{HCO}_3$  vs. chloride content, and by the different BEX index's spatial distribution in the two seasons. Regarding the fact that most salinized areas are relatively far from the coast, it can be said that higher salinity in boreholes of Temeke relatively far from the coast, is probably due to higher population densities and thus higher density of extraction wells, which is evidence of up-coning processes. Moreover, the highly salinized area of Temeke comprises the industrial district of the city, where the main manufacturing centers are located. This suggests that a further stress is applied on groundwater resources in this area. In addition, in Temeke most of the coastal area is covered by vegetation, and there are no boreholes analyzed in close proximity of the coastal area.

## References

- Al Farrah, N., K. Martens, and K. Walraevens. 2011. Hydrochemistry of the upper miocene-pliocene-quaternary aquifer complex of Jifarah plain, NW-Libya. *Geologica Belgica*.
- Civita M. et al. 1999. Una metodologia GIS per la valutazione della ricarica attiva degli acquiferi. *Quaderni di Geologia Applicata* 1.
- Congedo, L., M. Munafò, and S. Macchi. 2013. Investigating the relationship between land cover and vulnerability to climate change in Dar es Salaam. Working paper ACC DAR Sapienza University of Rome. <http://www.planning4adaptation.eu/>. Accessed 4 Dec 2015.
- Custodio, E. 1987. Groundwater problems in coastal areas. A contribution to the International hydrological programme. Paris: UNESCO.
- Rhoades, J.D, A. Kandiah, and A.M. Mashali. 1992. The use of saline waters for crop production. FAO irrigation and drainage paper 48. <http://www.fao.org/docrep/T0667E/t0667e00.htm#Contents>.
- Mjemah, I.C. 2007. Hydrogeological and hydrogeochemical investigation of a coastal aquifer in Dar es Salaam, Tanzania. Ghent: Ghent University, Ph.D. thesis.
- Mtoni, Y., I.C. Mjemah, C. Bakundukize, M. Van Camp, K. Martens, and K. Walraevwns. 2013. Saltwater intrusion and nitrate pollution in the coastal aquifer of Dar Es Salaam, Tanzania.

- Mtoni, Y., I.C. Mjemah, K. Msindai, M. Van Camp, and K. Walraven. 2012. Saltwater intrusion in the Quaternary aquifer of the Dar es Salaam region, Tanzania.
- Sappa G., A. Trotta, S. Vitale. in press. Climate change impact on groundwater active recharge in coastal plain of Dar es Salam (Tanzania). IAEG XII Congress, Turin, September 15–19, 2014.
- Sappa, G., S. Vitale, M.T. Coviello, G. Faldi, and M. Rossi. 2013a. Analysis of the sensitivity to seawater intrusion of Dar es Salaam's coastal aquifer with regard to climate change. Working paper, Rome: Sapienza University: <http://www.planning4adaptation.eu>.
- Sappa, G., F. Ferranti, S. Ergul, and G. Ioanni. 2013b, Evaluation of the groundwater active recharge trend in the coastal plain of Dar es Salaam (Tanzania). *Journal of Chemical and Pharmaceutical Research* 5(12): 548–552.
- Sappa G., F. Ferranti, G. Luciani. 2013c. Effects of precipitations on groundwater salinization in Dar Es Salaam coastal plain (Tanzania), International conference on Frontiers of environment, energy and bioscience-ICFEEB 2013.
- Stuyfzand, P.J. 1989. A new hydrochemical classification of water types. *J. Regional Characterization of Water Quality*, Proceedings of the Baltimore symposium, IAHS 182.
- Stuyfzand, P.J. 1992. Behaviour of major and trace constituents in fresh and salt intrusion waters, in the western Netherlands. Proceedings 12th salt water intrusion meeting, Barcelona, nov.
- Van Camp, M., I.C. Mjemah, N. Al Farrah, and K. Walraevens. 2012. Modeling approaches and strategies for data - scarce aquifers: example of the Dar es Salaam aquifer in Tanzania. *Hydrogeology Journal* 21(2) 341–356.
- Van Camp, M., and K. Walraevens. 2004. Advances in understanding natural groundwater quality controls in coastal aquifers 18 SWIM. Cartagena, Spain: Ed. Araguàs, Custodio and Manzano.
- World Health Organization. 2003. *WHO guidelines for drinking-water quality*.
- World Meteorological Organization. 2011. *Guide to climatological practices*.